Ultrasonics Sonochemistry 18 (2011) 901–906

Contents lists available at ScienceDirect

Ultrasonics Sonochemistry

journal homepage: www.elsevier.com/locate/ultsonch

Effect of reaction conditions on size and morphology of ultrasonically prepared $Ni(OH)_2$ powders

S. Cabanas-Polo [a,*], K.S. Suslick [b], A.J. Sanchez-Herencia [a]

[a] Instituto de Cerámica y Vidrio (CSIC), C/Kelsen, 5, 28049 Madrid, Spain
[b] School of Chemical Sciences, University of Illinois, 600 S, Mathews Avenue, Urbana, IL 61801, USA

ARTICLE INFO

Article history:
Received 29 September 2010
Accepted 26 November 2010
Available online 4 December 2010

Keywords:
Powders
Synthesis
Sonochemistry
Nickel hydroxide
Ammonia complexes

ABSTRACT

Modern electrochemical devices require the morphological control of the active material. In this paper the synthesis of nickel hydroxide, as common active compound of such devices, is presented. The influence of ultrasound in the synthesis of nickel hydroxide from aqueous ammonia complexes is studied showing that ultrasound allows the fabrication of flower-like particles with sizes ranging in between 0.7 and 1.0 μm in contrast with the 6–8 μm particles obtained in the absence of ultrasound. The influence of gas flow, temperature of the process and surfactants in the ultrasonically prepared powders is discussed in term of shape, size and agglomeration of the particles. Adjusting the experimental condition, spherical or platelet-like particles are obtained with sizes ranging from 1.3 μm to 200 nm.

1. Introduction

Nickel hydroxide has received increasing attention in the past few decades due to its use as the active material in the positive electrode of alkaline rechargeable batteries [1–6] and as the most common precursor of nickel oxide, which is widely used as a hydrogenation catalyst and in the ceramic industry for sintered fritz and glazes. The effectiveness of $Ni(OH)_2$ for these applications depends highly on the size and morphology of the active material. For example, it has been demonstrated that the addition of 8 wt.% of nanoparticles to a micrometer phase of nickel hydroxide, increases the capacity of alkaline rechargeable batteries electrodes by 14% due to closer packing as the nanometer particles take up free spaces between micrometer ones, which increases the proton diffusion through the material [1,2]. The capability of fabricate powders with a specific morphology and small particle size is also important for producing metallic nanoparticles for ceramic matrix reinforcement or incorporation to catalytic devices [7–9].

Nickel hydroxide presents two polymorphs, α-$Ni(OH)_2$ and β-$Ni(OH)_2$. Although the alpha phase presents higher theoretical electrochemical capacity [5], it is a metastable turbostratic phase that rapidly changes to the beta phase during synthesis or in strong alkali media [10]. The beta phase is therefore a better candidate as battery cathode material. The beta phase (teophrastite), is a hexagonal phase isostructural with brucite ($Mg(OH)_2$) that presents an interlaminar distance of c = 4.605 Å and Ni–Ni distance of a = 3.126 Å.

The most common methods for obtaining beta nickel hydroxide involve either chemical precipitation from nickel salts [11,12] or hydrothermal synthesis [13–15]. For example, Meyer et al. reported the synthesis of nickel hydroxide powder with different sizes and morphologies depending on the precipitation agent and the molar ratio (base/metal) [11] and Liang et al. studied the influence of pH and reaction time during hydrothermal synthesis on those parameters in order to achieve homogeneous products [13]. Sonochemical synthesis of metal hydroxides has also been reported [16–20]. Jeevanandam et al. prepared α-$Ni(OH)_2$ by a urea method assisted by ultrasound [18] and Vidotti et al. synthesized nickel hydroxide nanoparticles by a sonochemical method for electrochromic devices [20]. The chemical effects of ultrasound originate primarily from the phenomena of acoustic cavitation, i.e. the formation, growth and subsequent implosive collapse of microbubbles within the liquid. The generally accepted "hot spot" mechanism of sonochemistry arises from the compressional heating that bubble collapse induces, which produces extraordinary conditions inside the bubble. Measured temperatures of about 5000 K, pressures of approximately 1000 atm and cooling rates of $\geqslant 10^{11}$ K/s are created [21,22] and these are responsible for the subsequent chemical reactions that have found important uses in materials chemistry [23–25].

In this work we present the sonochemical synthesis of β-$Ni(OH)_2$ from simple aqueous ammonia complexes of nickel. The effects of the temperature of the reaction media and a gas flow above the solution on the morphology and particle size have been studied. The employment of cationic (polyvinylpyrrolidone), anionic (polyacrylic acid) and neutral (poly[vinyl alcohol]) surfactants has also been considered in order to further control the particle size and to obtain well dispersed powders.

* Corresponding author. Tel.: +34 917355840; fax: +34 917355843.
E-mail addresses: scabanas@icv.csic.es (S. Cabanas-Polo), ksuslick@illinois.edu (K.S. Suslick), ajsanchez@icv.csic.es (A.J. Sanchez-Herencia).

1350-4177/$ - see front matter © 2010 Elsevier B.V. All rights reserved.
doi:10.1016/j.ultsonch.2010.11.017

2. Experimental

2.1. Synthesis of β-$Ni(OH)_2$

Nickel nitrate hexahydrate ($Ni(NO_3)_2{\cdot}6H_2O$; Panreac Química S.A.U., Spain) and ammonium hydroxide (Panreac Química S.A.U., Spain) were used as reactants. A high intensity ultrasonic horn (Ti horn, 24 kHz, 50 W/cm^2, UP400S, Dr. Hielsecher, Germany) was used as the source of ultrasound. An appropriate amount of $Ni(NO_3)_2{\cdot}6H_2O$ ($[Ni^{2+}]_{solution}$ = 0.1 mol L^{-1}) was first dissolved in a 2 mol L^{-1} ammonium solution to form stable nickel ammonia complexes ($Ni(NH_3)_x^{2+}$) that were then sonicated for 90 min. Original synthesis was performed using regular glassware (open system) cooled in an ice/water bath (sample NH). Nickel hydroxide powders were also synthesized in absence of ultrasound by heating the nickel ammonia complexes solution for 2 h at 60 °C in regular glassware under magnetic stirring. This sample was used as reference (sample NHR) to establish the effect of ultrasound during the process.

Powders obtained were filtered using polymeric filters (ø = 0.22 μm), washed with distilled water at pH ∼ 10 (adjusted with tetramethyl ammonium hydroxide) and dried at 60 °C for 2 h. XRD analysis was performed using a Siemens-Bruker D5000 diffractometer (Germany, Kα(Cu) λ = 1.5405 Å; 40 kV; 30 mA; 2θ = 10–70). The size and morphology of the powders were examined by FE-SEM Hitachi S-4700 microscope (Japan). Density and specific surface area were measured using a Monosorb Multipycnometer and a Monosorb Surface Area from Quantachrome Corporation (USA). Average particles sizes were calculated directly from FE-SEM micrographs by measuring two perpendicular diagonals of the particles.

2.2. Effect of gas flow rate, temperature and surfactants

The influence of a gas flow rate was studied using two different compress air flow rates, 0.4 and 0.6 standard liter per minute (slpm), (samples NHAF0.4 and NHAF0.6, respectively), and a sealed Suslick cell (closed system). Influence of temperature was evaluated for both, open and sealed systems using a thermostat. Four different samples were obtained: two in an open system at 5 and 40 °C (samples NHT5 and NHT40, respectively) and two more in sealed system at 10 and 20 °C under an air flow rate of 0.4 slpm (samples NHAFT10 and NHAFT20, respectively). Finally, the effects of three different surfactants (polyacrylic acid (PAA, polyacrylic M_w 5100 sodium salt, Fluka, USA), polyvinylpyrrolidone (PVP, average M_w ca. 29,000, Aldrich, USA) and poly(vinyl alcohol) (PVA, typical M_w 31,000–50,000, Sigma–Aldrich, USA)) were tested by their addition to the starting solution at a rate of 0.11 ml/min during sonication (samples NHPAA, NHPVP, NHPVA, respectively). Surfactant solutions were prepared in water or ethanol and in all cases 2 wt.% of each surfactant relative to $Ni(OH)_2$ was added during reaction.

3. Results and discussion

3.1. Synthesis of β-$Ni(OH)_2$

Chemical stability of nickel ammonia complexes ($Ni(NH_3)_x^{2+}$) was studied using equilibrium diagrams with MEDUSA software (http://www.kemi.kth.se/medusa) and the hydrochemical equilibrium-constant database (HYDRA) in order to establish the experimental conditions. Fig. 1 shows pH vs log [NH_3] predominance area diagram for a fixed nickel ion concentration of 0.1 mol L^{-1}. Experimentally, for [NH_3] = 2 mol L^{-1} and [Ni^{2+}] = 0.1 mol L^{-1}, the pH of the solution reaches a value of approximately 11, where $Ni(NH_3)_6^{2+}$ is the predominant specie. At this point, if ammonia concentration decreases, the pH also decreases leading the precipitation of nickel hydroxide. In this experiment the decrease in ammonia concentration is induced by the effects of ultrasound: ultrasonic degassing occurs due to growth and coalescence of bubbles generated during cavitation, in this case depleting the concentration of dissolved ammonia in the liquid and inducing precipitation of nickel hydroxide.

Prior to any change within the media, reference samples was synthesized by thermal treatment of the ammonia complexes solution. These samples were labeled as NHR and the synthesis yields were about 60%. In the case of samples obtained in the presence of ultrasound (labeled NH), the yield was 27%.

Fig. 2 shows the XRD pattern of the as-prepared powders obtained with and without ultrasound. Both samples were characterized as pure β-$Ni(OH)_2$ (indexed using the JCPDS card 14-0117) and present a hexagonal structure with well defined peaks and an interlaminar distance of 4.59 Å. It can be seen that sample NH presents broader peaks than sample NHR what is related to smaller particle size since the higher the peak width, the smaller the crystallite size [26]. From peak position and full width at half maximum (FWHM) of (0 0 1) reflection, the crystallite size along the *c*-axis (L_{hkl}) was calculated using the Warren modification of Scherrer formula,

$$L_{hkl} = \frac{K\lambda}{\Delta(2\theta)\cos(\theta)} \quad (1)$$

where $\Delta(2\theta)$ is the FWHM of a given peak [hkl] (in radians), λ is the wave length used (in Å), θ is half the scattering angle (in radians) and K is the Scherrer constant that takes into account the symmetry of the crystals (K is equal to 0.94 for [0 0 l] reflections and 1.84 for [hk0] ones) [11]. Results of crystallite size are shown in Table 1 along with other morphological characteristics such as density, specific surface area and BET diameter for both powders.

Both the effective, BET diameter (calculated using specific surface area and density values) and size estimated from L_{hkl} show again that sample NH has a significantly smaller particle size than the reference sample. When applying ultrasound to the starting solution, homogeneous nucleation occurs and is followed by the growth of the particles and subsequent aggregation. The shockwaves in the liquid created by the high energy process of sonication is sufficient to break some of the aggregates but does not allow the primary particles to remain independently in solution

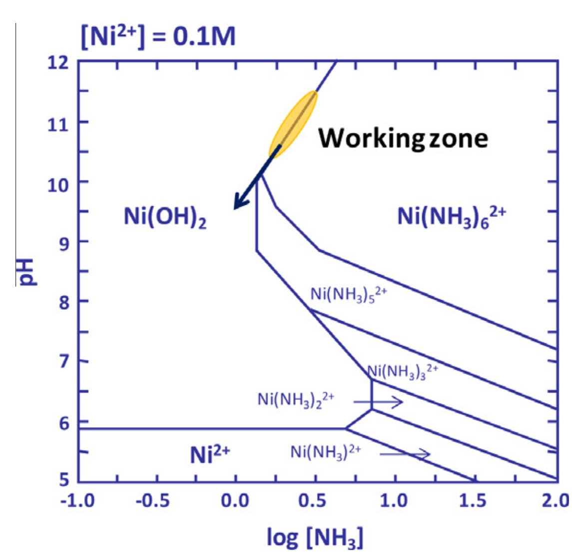

Fig. 1. pH vs log [NH_3] predominance area diagram for a fixed [Ni^{2+}] = 0.1 mol L^{-1}.

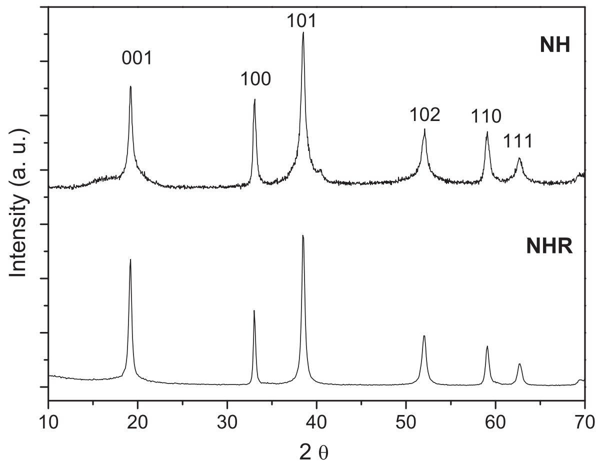

Fig. 2. XRD patterns of samples NH (upper) and NHR (lower) samples. Both powders correspond to the β-$Ni(OH)_2$ phase.

Table 1
Crystallite size across the *c*-axis, density, specific surface area and BET diameter of synthesized nickel hydroxide powders.

Sample	L_{hkl} (nm)	ρ (g/cm^3)	SSA (m^2/g)	D_{BET} (nm)
NH	13.9	3.9	30.3	51.0
NHR	23.7	3.8	20.8	75.9

[5]. FE-SEM images of sample NH (Fig. 3a) show flower-like particles with diameters between 0.75 and 1 μm composed of thin nanoplatelets of 50 nm thick (that corresponds to the theoretical BET diameter). In the case of sample NHR (Fig. 3b) large aggregates, in the range of 6–8 μm also made up of 50–100 nm thick nanoplatelets are obtained.

It has been stated that nucleation rate plays an important role in the morphology of the fabricated powders. For that reason, other factors affecting nucleation mechanism have been faced in the precipitation of nickel hydroxide assisted by ultrasound presented in this work. Gas flow rate and reaction temperature have been selected as synthesis variables. It must be noticed that temperature will affect not only the nucleation but also the growing processes of the particles.

3.2. Influence of gas flow rate

Fig. 4 shows the XRD patterns for samples obtained under air flow rates of 0.4 and 0.6 slpm (samples NHAF0.4 and NHAF0.6, respectively) that corresponds to the β-$Ni(OH)_2$ phase. The specific surface area was found to be 16.4 m^2/g for sample NHAF0.4 and 41.8 m^2/g for sample NHAF0.6. The increment in the specific surface area of sample NHAF0.6 corresponds to a reduction of the particle size, as can be observed in Fig. 5, where FE-SEM micrographs show large differences in this parameter, with sample NHAF0.6 much smaller (0.2 μm) than sample NHAF0.4 (0.5 μm). The degassing process, in which the nickel hydroxide precipitation is based in this experiment, is more efficient at higher gas flow and this decreases the ammonia concentration in solution more rapidly, which increases the nucleation rate of precipitation and produces smaller particle sizes. This result is also observed in the XRD patterns of Fig. 4 where peaks corresponding to sample NHAF0.6 seem to be broader than those of sample NHAF0.4.

3.3. Influence of temperature

The influence of temperature in the described synthesis has been studied using sealed and open systems. Temperatures of 10 and 20 °C for the sealed system (samples NHAFT10 and NHAFT20, respectively), and 5 and 40 °C for the open system (samples NHT5 and NHT40, respectively) were maintained constant around the reaction cell using a thermostatic bath. Temperature inside the cell, measured at the end of the experiments for synthesis under air flow rate (sealed system) was about 20° higher than the bath temperature while in the open system the final temperature rise was

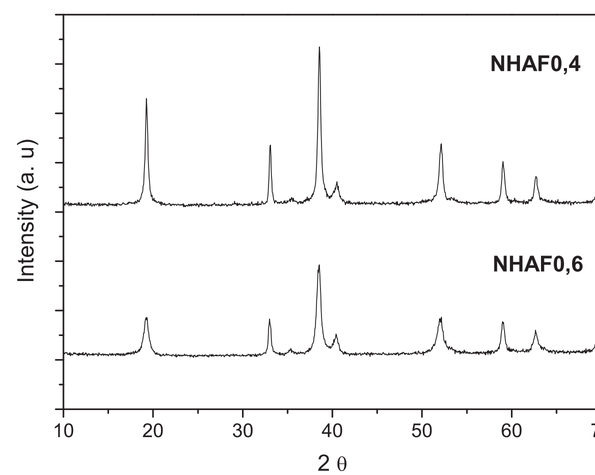

Fig. 4. XRD patterns of samples NHAF0.4 (upper) and NHAF0.6 (lower). Peaks at 2θ = 35 and 41 correspond to titanium from degradation of the ultrasonic tip horn.

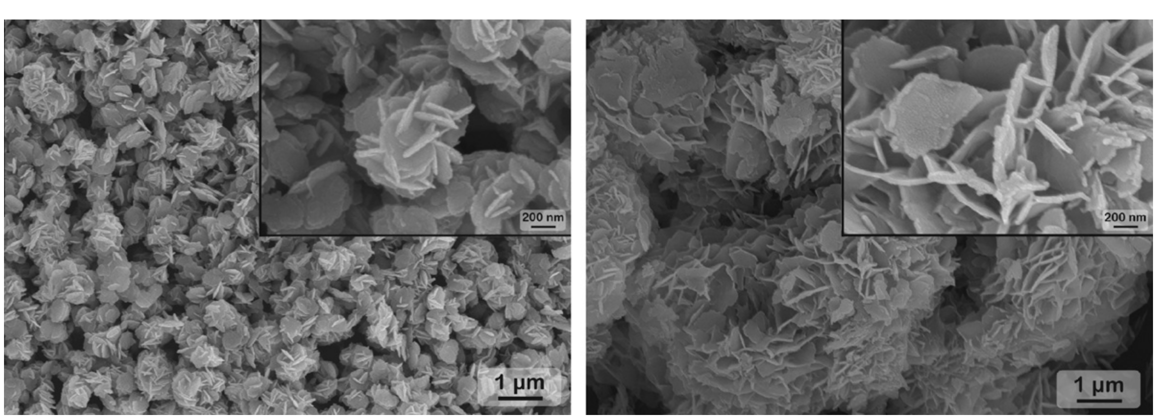

Fig. 3. FE-SEM images of β–$Ni(OH)_2$ synthesized with (left, sample NH) and without (right, sample NHR) ultrasound.

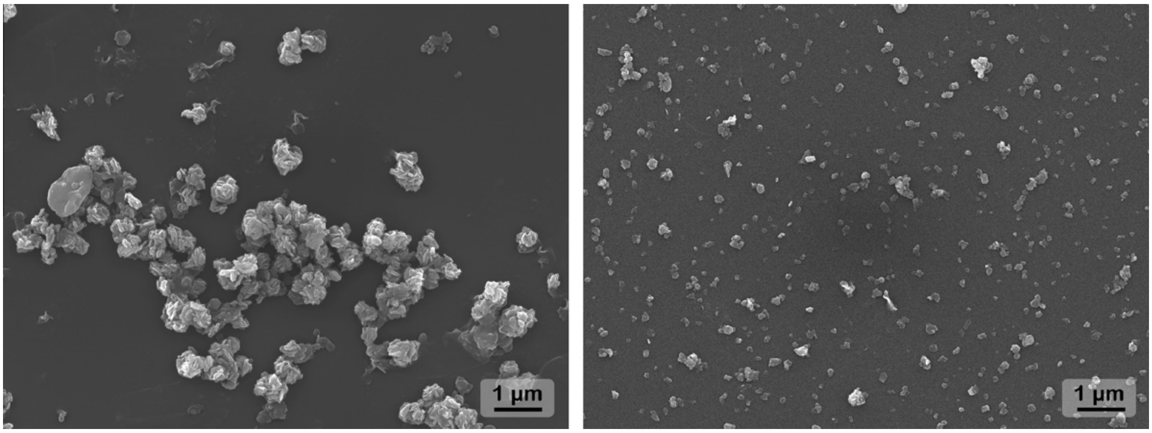

Fig. 5. FE-SEM images of samples NHAF0.4 (left) and NHAF0.6 (right).

around 30° higher. This is due to the forced cooling that gas flow imposes into the sealed system. Fig. 6 shows the FE-SEM images for the four samples. It can be clearly seen that as temperature increases, the aggregate size increases as well. Increasing temperature leads to a decrease in both surface tension and viscosity of the aqueous system at the time that vapour pressure increases. Therefore, bubbles will form more easily within the liquid [27]. This fact will increase the degassing process of the system and, hence, nucleation rate will also increase. An increase in temperature, along with the high energy achieved with ultrasound, increases the surface energy of the particles within the reaction media and so coalescence processes can occur, bringing the growth mechanism overcome the nucleation rate. From these results it can be considered that coalescence mechanism does not depend on gas flow and leads to a homogeneous growth that result in large spherical aggregates with rough surfaces and a narrow size distribution (Fig. 6b (sample NHAFT20) and d (sample NHT40)), in contrast with samples obtained at the lowest temperatures (Fig. 6a (samples NHAFT10) and c (sample NHT5)) where platelet-like structures are obtained. Particles sizes measured using image analysis were found to be around 0.2 and 0.4 µm for samples at the lowest temperatures (NHAFT10 and NHT5, respectively) and 0.8 and 1.3 µm for samples at the higher temperatures (samples NHAFT20 and NHT40, respectively).

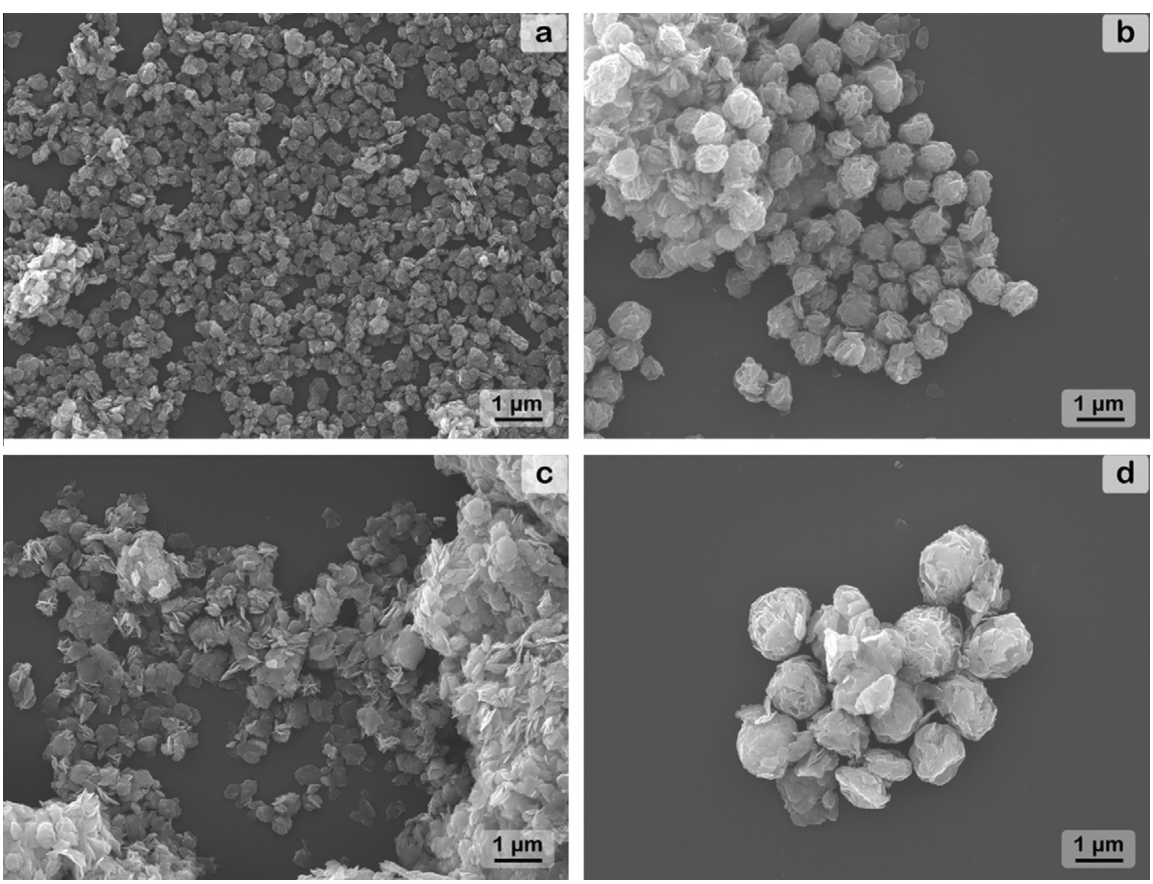

Fig. 6. FE-SEM images of samples (a) NHAFT10, (b) NHAFT20, (c) NHT5 and (d) NHT40.

3.4. Influence of surfactants

Noting that during synthesis small particles tend to agglomerate into larger ones that settle out of solution, surfactants were added to the synthesis media during sonication. Surfactants can act in two different ways when added to a synthesis media. On the one hand, these additives can control the particle size or promote preferential growth of the particles by blocking the crystal growth selectively. On the other hand, surfactants can stabilize the growing particles within the reaction media allowing the obtaining of well dispersed suspensions [11,28–32].

Three different surfactants have been chosen for this work: PAA (anionic), PVP (cationic) and PVA (neutral). PAA was chosen because it has been proved its capability as well dispersion agent in nickel oxide slurries and also for stabilization of metallic nanoparticles [32,33]. In the case of PVP, it is commonly used to stabilize metallic nanoparticles by the steric mechanism [34,35] and to control nickel powders morphology during synthesis [36], and the PVA has been previously used as binder in some ceramic systems for tape casting [37].

Although anionic PAA can act as a well dispersion agent in ceramic slurries stabilizing aqueous nickel oxide suspensions, when adding PAA as a synthesis aid in our system, no nickel hydroxide is obtained. According to Chou et al., PAA seems to form very stable complexes with nickel ions in solution inhibiting nickel hydroxide precipitation [32]. In contrast, the addition of cationic PVP or neutral PVA both do lead to the synthesis of β-$Ni(OH)_2$ (cf. XRD in Fig. 7) with platelet-like morphology, as shown in Fig. 8. The isolation of platelet-like particles instead of the flower-like ones could be a consequence of the strong preferential absorption of the surfactants on the 0 0 1 plane of nickel hydroxide structure among the steric effect of polymeric surfactants [34]. For both polymers the platelet-like structures show thicknesses lower than 50 nm and diameters lower than 1 μm.

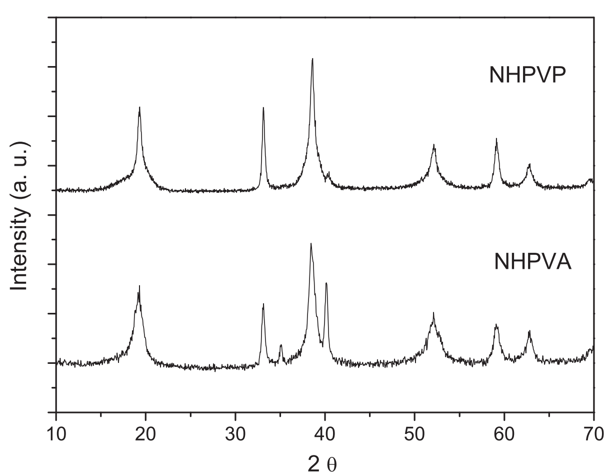

Fig. 7. XRD patterns of samples NHPVP (upper) and NHPVA (lower). Peaks at 2θ = 35 and 41 correspond to titanium from degradation of the ultrasonic tip horn.

4. Conclusions

In this work the synthesis of beta nickel hydroxide by a simple method based on the application of ultrasound to an aqueous solution of the nickel ammonia complexes has been presented. This method is faster than the traditional ones for nickel hydroxide synthesis and enables the facile isolation of pure products. Powders obtained under ultrasonic radiation have smaller particle sizes (around 0.75 μm) with a narrower particle size distribution than powders obtained in silence conditions where particles of several microns are obtained.

Effects of environmental variables in the synthesis of $Ni(OH)_2$ assisted by ultrasound have also been studied. It has been observed that by controlling the external atmosphere (by flushing with a controlled air flow rate), smaller particle sizes are obtained. In this sense, an air flow rate of 0.6 slpm decreases the particle size to 200 nm. The influence of temperature reveals that, independently of the gas flow, by increasing the reaction temperature, a coalescence mechanism leads to formation of larger aggregates at the time that particle morphology changes from platelet-like to spheres.

Three different polymeric surfactants have been used as synthesis aids. It has been observed that the use of anionic PAA inhibits the nickel hydroxide precipitation. Nevertheless, cationic PVP and neutral PVA allow the nickel hydroxide precipitation with platelet-like morphology although no significant changes in particle size are observed. The obtaining of planar platelet-like morphologies when using PVP and PVA may be due in part to the steric effect of polymeric surfactants and to the preferential absorption of polymers on a specific plane of nickel hydroxide structure.

Acknowledgments

The authors would like to acknowledge the Spanish Government support under Project MAT 2009-14448-C02-01 and the Frederick Seitz Materials Research Laboratory Central facilities, University of Illinois, which are partially supported by the US Department of Energy under grants DE-FG02-07ER46453 and DE-

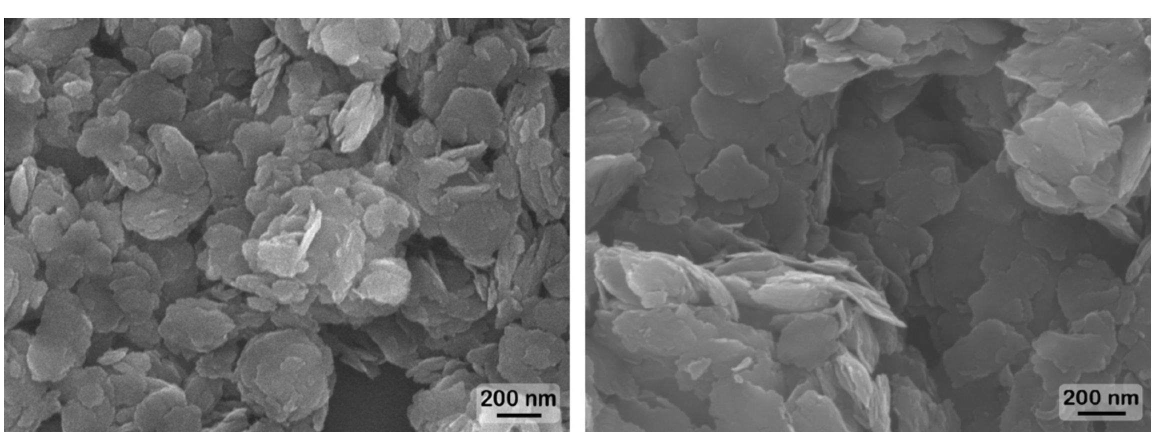

Fig. 8. FE-SEM images of samples NHPVP (left) and NHPVA (right).

FG02-07ER46471. Sandra Cabanas Polo acknowledges the JAE-Predoc 2008 Program for supporting her stay at the University of Illinois at Urbana-Champaign.

References

[1] X. Han, X. Xie, C. Xu, D. Zhou, Y. Ma, Morphology and electrochemical performance of nano-scale nickel hydroxide prepared by supersonic coordination–precipitation method, Opt. Mater. 23 (2003) 465–470.
[2] X. Liu, L. Yu, Influence of nanosized $Ni(OH)_2$ addition on the electrochemical performance of nickel hydroxide electrode, J. Power Sources 128 (2004) 326–330.
[3] M.R. Palacin, Recent advances in rechargeable battery materials: a chemist's perspective, Chem. Soc. Rev. 38 (2009) 2565–2575.
[4] G. Sakai, M. Miyazaki, T. Kijima, Synthesis of β-$Ni(OH)_2$ hexagonal plates and electrochemical behavior as a positive electrode material, J. Electrochem. Soc. 157 (2010) A932–A939.
[5] M.A. Kiani, M.F. Mousavi, S. Ghasemi, Size effect investigation on battery performance: comparison between micro- and nano-particles of β-$Ni(OH)_2$ as nickel battery cathode material, J. Power Sources 195 (2010) 5794–5800.
[6] H. Wang, H.S. Casalongue, Y. Liang, H. Dai, $Ni(OH)_2$ nanoplates grown on graphene as advanced electrochemical pseudocapacitor materials, J. Am. Chem. Soc. 132 (2010) 7472–7477.
[7] J.S. Moya, S. Lopez-Esteban, C. Pecharroman, The challenge of ceramic/metal microcomposites and nanocomposites, Prog. Mater. Sci. 52 (2007) 1017–1090.
[8] G. Boschloo, A. Hagfeldt, Spectroelectrochemistry of nanostructured NiO, J. Phys. Chem. B 105 (2001) 3039–3044.
[9] W.-H. Tuan, J.-R. Chen, T.-J. Yang, Minimum amount of nano-sized nickel particles to enhance the strength of alumina, J. Eur. Ceram. Soc. 27 (2007) 4705–4709.
[10] A. Delahaye-Vidal, M. Figlarz, Textural and structural studies on nickel hydroxide electrodes. II. Turbostratic nickel (II) hydroxide submitted to electrochemical redox cycling, J. Appl. Electrochem. 17 (1987) 589–599.
[11] M. Meyer, A. Bee, D. Talbot, V. Cabuil, J.M. Boyer, B. Repetti, R. Garrigos, Synthesis and dispersion of $Ni(OH)_2$ platelet-like nanoparticles in water, J. Colloid. Interf. Sci. 277 (2004) 309–315.
[12] Q. Song, Z. Tang, H. Guo, S.L.I. Chan, Structural characteristics of nickel hydroxide synthesized by a chemical precipitation route under different pH values, J. Power Sources 112 (2002) 428–434.
[13] Z.-H. Liang, Y.-J. Zhu, X.-L. Hu, ß-nickel hydroxide nanosheets and their thermal decomposition to nickel oxide nanosheets, J. Phys. Chem. B 108 (2004) 3488–3491.
[14] M.-G. Ma, J.-F. Zhu, J.-X. Jiang, R.-C. Sun, Hydrothermal-polyol route to synthesis of β-$Ni(OH)_2$ and NiO in mixed solvents of 1,4-butanediol and water, Mater. Lett. 63 (2009) 1791–1793.
[15] E. Zhang, Y. Tang, Y. Zhang, C. Guo, L. Yang, Hydrothermal synthesis of β-nickel hydroxide nanocrystalline thin film and growth of oriented carbon nanofibers, Mater. Res. Bull. 44 (2009) 1765–1770.
[16] M.A. Alavi, A. Morsali, Syntheses and characterization of $Mg(OH)_2$ and MgO nanostructures by ultrasonic method, Ultrason. Sonochem. 17 (2010) 441–446.
[17] M.A. Alavi, A. Morsali, Syntheses and characterization of $Sr(OH)_2$ and $SrCO_3$ nanostructures by ultrasonic method, Ultrason. Sonochem. 17 (2010) 132–138.
[18] P. Jeevanandam, Y. Koltypin, A. Gedanken, Synthesis of nanosized α-nickel hydroxide by a sonochemical method, Nano. Lett. 1 (2001) 263–266.
[19] A. Askarinejad, A. Morsali, Synthesis of cadmium(II) hydroxide, cadmium(II) carbonate and cadmium(II) oxide nanoparticles; investigation of intermediate products, Chem. Eng. J. 150 (2009) 569–571.
[20] M. Vidotti, C. Van Greco, E.A. Ponzio, S.I. Cordoba De Torresi, Sonochemically synthesized $Ni(OH)_2$ and $Co(OH)_2$ nanoparticles and their application in electrochromic electrodes, Electrochem. Commun. 8 (2006) 554–560.
[21] K.S. Suslick, D.A. Hammerton, R.E. Cline Jr., The sonochemical hot spot, J. Am. Ceram. Soc. 108 (1986) 5641–5642.
[22] K.S. Suslick, D.J. Flannigan, Inside a collapsing bubble: sonoluminescence and the conditions during cavitation, Annu. Rev. Phys. Chem. (2008) 659–683.
[23] J.H. Bang, K.S. Suslick, Applications of ultrasound to the synthesis of nanostructured materials, Adv. Mater. 22 (2010) 1039–1059.
[24] K.S. Suslick, G.J. Price, Applications of ultrasound to materials chemistry, Annu. Rev. Matl. Sci. (1999) 295–326.
[25] A. Gedanken, Using sonochemistry for the fabrication of nanomaterials, Ultrason. Sonochem. 11 (2004) 47–55.
[26] H. Zhou, Z. Zhou, Preparation, structure and electrochemical performances of nanosized cathode active material $Ni(OH)_2$, Solid State Ionics 176 (2005) 1909–1914.
[27] J. Mason, J.P. Lorimer (Eds.), General Principles, Applied Sonochemistry. The Uses of Power Ultrasound in Chemistry and Processing, Wiley-VCH Verlag, Weinheim, 2002. pp. 25–60.
[28] D. Andeen, J. Kim, F. Lange, G. Goh, S. Tripathy, Lateral epitaxial overgrowth of ZnO in water at 90 °C, Adv. Funct. Mater. 16 (2006) 799–804.
[29] F. Herranz, M. Morales, A. Roca, M. Desco, J. Ruiz-Cabello, A new method for the rapid synthesis of water stable superparamagnetic nanoparticles, Chem.-Eur. J. 14 (2008) 9126–9130.
[30] J. Kim, D. Andeen, F. Lange, Hydrothermal growth of periodic, single-crystal ZnO microrods and microtunnels, Adv. Mater. 18 (2006) 2453–2457.
[31] L. Piao, K.H. Lee, W.J. Kwon, S.-H. Kim, S. Yoon, The simple and facile methods to improve dispersion stability of nanoparticles: different chain length alkylcarboxylate mixtures, J. Colloid Interf. Sci. 334 (2009) 208–211.
[32] K.-S. Chou, K.-C. Huang, Studies on the chemical synthesis of nanosized nickel powder and its stability, J. Nanopart. Res. 3 (2001) 127–132.
[33] A.J. Sanchez-Herencia, N. Hernandez, R. Moreno, Rheological behavior and slip casting of Al_2O_3–Ni aqueous suspensions, J. Am. Ceram. Soc. 89 (2006) 1890–1896.
[34] Z. Zhang, B. Zhao, L. Hu, PVP protective mechanism of ultrafine silver powder synthesized by chemical reduction processes, J. Solid State Chem. 121 (1996) 105–110.
[35] Z.Y. Wu, C.M. Liu, L. Guo, R. Hu, M.I. Abbas, T.D. Hu, H.B. Xu, Structural characterization of nickel oxide nanowires by X-ray absorption near-edge structure spectroscopy, J. Phys. Chem. B 109 (2005) 2512–2515.
[36] Y. Luo, J.-C. Zhang, Y. Shen, S.-T. Jiang, G.-Y. Liu, L.-J. Wang, Preparation and magnetic properties of nickel nanorods by thermal decomposition reducing methods, T. Nonferr. Metal. Soc. 16 (2006) s96–s100.
[37] S. Ramanathan, K.P. Krishnakumar, P.K. De, S. Banerjee, Powder dispersion and aqueous tape casting of YSZ–NiO composite, J. Mater. Sci. 39 (2004) 3339–3344.